

05/12/2025

ENDOTARGET/ REPORT ON EFFECT OF LPS, OMVs AND ECVs ON ON-CHIP BASED GUT BARRIER INTEGRITY

WP2, Task 2.6

DELIVERABLE VERSION:

D2.5, V1.1

DISSEMINATION LEVEL:

PU

AUTHOR(S):

Martin Frauenlob

ENDOTARGET

¹PU = Public - fully open

SEN = Sensitive - limited under the conditions of the Grant Agreement

EU classified –RESTREINT-UE/EU-RESTRICTED, CONFIDENTIEL-UE/EU-CONFIDENTIAL, SECRET-UE/EU-SECRET under Decision 2015/444

DOCUMENT HISTORY

PROJECT ACRONYM	ENDOTARGET		
Project Title	Systemic Endotoxemia as the driver of chronic inflammation -Biomarkers and novel therapeutic targets for Arthritis		
Grant Agreement No	101095084		
Project Coordinator	HUS		
Project Duration	01/01/2023 – 31/12/2026		
Deliverable No.	2.4		
Diss. Level	Public		
Deliverable Lead	Martin Frauenlob (TUW)		
Status	Working		
	Verified by other WPs/Partners		
	X	Final Version	
Due date	31/12/2025		
Submission date	23/12/2025		
Work Package	WP2		
Work Package Lead	Francesco Ciccia (UNICAM)		
Contribution Beneficiary(ies)	TUW, UH, UNICAM, HUS		
DoA			
DATE	VERSION	AUTHOR	COMMENT
05/12/2025	0.1	Martin Frauenlob	First draft
05/12/2025	0.2	Reetta Satokari	Editing and review
19/12/2025	0.3	Antonio Ciancio	Editing and review
19/12/2025	1.0	Martin Frauenlob	Review
23/12/2025	1.1	Barreto, Gonçalo, Martin Frauenlob	Editing and review

©2023–2026 ENDOTARGET Consortium Partners. All rights reserved.

Funded by the European Union. Views and opinions expressed are however those of the author(s) only and do not necessarily reflect those of the European Union. Neither the European Union nor the granting authorities can be held responsible for them.

ENDOTARGET is a Horizon Europe project supported by the European Commission under grant agreement No 101095084 and it is supported by the Swiss State Secretariat for Education, Research and Innovation (SERI) under contract number 22.00462. All information in this deliverable may not be copied or duplicated in whole or part by any means without express prior agreement in writing by the ENDOTARGET partners. All contents are reserved by default and may not be disclosed to third parties without the written consent of the ENDOTARGET partners, except as mandated by the Grant Agreement with the European Commission, for reviewing and dissemination purposes. All trademarks and other rights on third party products mentioned in this document are acknowledged and owned by the respective holders. The ENDOTARGET consortium does not guarantee that any information contained herein is error-free, or up-to-date, nor makes warranties, express, implied, or statutory, by publishing this document. For more information on the project, its partners and contributors, please see the ENDOTARGET website (<https://endotargetproject.eu/>).

EXECUTIVE SUMMARY

The ENDOTARGET project investigates the mechanistic links between gut microbiota-derived compounds, intestinal permeability, and systemic endotoxemia in rheumatic diseases (RDs), focusing on osteoarthritis (OA), rheumatoid arthritis (RA), and spondylarthritis (SpA). This deliverable (D2.5) reports on the development and validation of a microfluidic gut-on-a-chip platform to assess the impact of lipopolysaccharides (LPS) and bacterial membrane vesicles (BMV) such as outer membrane vesicles (OMVs), and extracellular vesicles (ECVs) on gut barrier integrity and immune responses.

Using a triple-coculture model of Caco-2 enterocytes, HT-29-MTX-E12 mucus-producing cells, and THP-1-derived macrophages, we evaluated acute and chronic exposure scenarios. While inflammatory cytokines significantly impaired barrier function, LPS and BMVs did not directly reduce transepithelial electrical resistance (TEER) or increase permeability. However, both induced robust IL-8 secretion, indicating pro-inflammatory signaling without compromising physical barrier integrity. Tolerogenic Bacteroidales compounds did not neutralize these effects.

The platform's bioimpedance sensors enabled real-time monitoring of barrier dynamics, complemented by cytokine profiling and permeability assays. This system provides a physiologically relevant tool for studying host-microbe interactions, advancing our understanding of endotoxemia drivers in RDs. Future studies will leverage this model to screen therapeutic interventions targeting microbial-induced inflammation and barrier dysfunction.

TABLE OF CONTENT

1	Introduction.....	8
2	Methods	9
2.1	Microfluidic chip fabrication.....	9
2.2	Human epithelial cell lines.....	10
2.3	Characterisation of the Intestinal Barrier Integrity off-chip.....	11
2.4	Proinflammatory capacity of inflammatory cytokine	13
2.5	Pro- inflammatory and tolerogenic capacity of LPS and BMVs.....	14
2.6	LPS and BMV competition assay	14
3	Results.....	16
3.1	Establishment of the epithelial Barrier on chip.....	16
3.2	Establishing the Acute and chronic LPS and BMVs exposure scenarios.....	19
3.3	Effect of LPS and BMVs on the Barrier Integrity on and off-chip	21
4	Conclusions.....	27
5	References.....	28

LIST OF FIGURES

Figure 1: Schematics of the organ-on-a-chip model.....	16
Figure 2: Establishing the epithelial co-culture ratio.....	17
Figure 3: Evaluation of Caco2/Ht19-MTX on-chip co-culture.....	19
Figure 4: Establishing the acute and chronic scenario.....	20
Figure 5: Effect of RD-associated and tolerogenic BMVs in an acute and chronic off-chip setup.....	22
Figure 6: Effect of RD-associated and tolerogenic BMVs in an acute on-chip setup.....	23
Figure 7: Effect of RD-associated and tolerogenic LPS in an acute and chronic off-chip setup.....	24
Figure 8: Effect of RD-associated and tolerogenic LPS in both acute and chronic on-chip setup.	25
Figure 9: Impact of LPS exposure on intestinal tri-culture barrier integrity and immune response.	26

LIST OF ABBREVIATIONS

ACRONYM	DESCRIPTION
A4N	L-alanine-4-nitroanilide hydrochloride
ATCC	American Type Culture Collection
BMV	bacterial membrane vesicles
DMEM	Dulbecco's modified Eagle's Medium
ECV	extracellular vesicle
FBS	fetal bovine serum
IC1	inflammatory cytokine 1
LPS	lipopolysaccharides
mucus	acidic mucopolysaccharides
OA	osteoarthritis
OMV	outer membrane vesicles
PDMS	polydimethylsiloxane
PET	polyethylene terephthalate
PFA	paraformaldehyde
p-NA	p-nitroanilide
PVA	polyvinyl alcohol
qPCR	quantitative polymerase chain reaction
RA	rheumatoid arthritis
RD	rheumatic diseases
RT	room temperature
SE	systemic endotoxemia
SpA	spondylarthritis
TEER	transepithelial electrical resistance
TLR4	toll-like receptor 4
TW	Transwell
ZO-1	zonula occludens-1

1 INTRODUCTION

Rheumatic diseases (RDs), including OA, RA, and SpA, are leading causes of disability and impose a significant economic burden worldwide. Growing evidence implicates gut microbiota dysbiosis and intestinal barrier dysfunction in the pathogenesis of chronic inflammation and systemic endotoxemia (SE). Bacteria-derived compounds, such as lipopolysaccharides (LPS) and bacterial membrane vesicles (BMVs), translocate across compromised epithelial barriers, triggering immune activation via Toll-like receptor 4 (TLR4) and other innate pathways.

The ENDOTARGET project aims to elucidate these mechanisms using advanced in vitro models. This deliverable describes the establishment of a microfluidic gut-on-a-chip system to evaluate the acute and chronic effects of LPS, OMVs, and ECVs on barrier integrity and immune responses. The platform integrates a triple-coculture of Caco-2, HT-29-MTX-E12, and THP-1-derived macrophages, replicating key features of the intestinal epithelium and immune surveillance.

Deliverable D2.5 is associated with work in Task 2.6 led by TUW who developed the microfluidic platform with integrated bioimpedance sensors, and in partnership with UH for bacterial compound isolation and characterization, UNICAM for immune response analyses, and HUS for clinical context. We assessed barrier function via bioimpedance measurements, fluorescence-based permeability assays, and cytokine quantification. Our findings reveal that while LPS and BMVs do not directly disrupt barrier tightness, they potently induce pro-inflammatory cytokine release, suggesting their role in immune activation rather than physical barrier disruption. This model provides a transformative tool for studying gut-joint axis interactions and identifying therapeutic targets to mitigate endotoxemia-driven inflammation in RDs.

2 METHODS

2.1 MICROFLUIDIC CHIP FABRICATION

2.1.1 Gut-on-a-chip platform with integrated gold electrodes

Microfluidic chip fabrication and development of gold electrodes was performed as described elsewhere [1], [2]. Briefly, for the fabrication of gold electrodes, porous polyethylene terephthalate (PET) membranes (3 μm pore size, 9 μm thickness) were first cleaned with distilled water and isopropanol, then dried at 120 °C. The membranes were then reversibly attached to microscope slides using a spin-coated layer of low-molecular-weight polyvinyl alcohol (PVA) and gradual heating to prevent wrinkles. A two-layer photoresist system was then applied, starting with LOR3A, followed by LNR-003, and each was soft-baked. The desired electrode geometry was transferred onto the resist via UV exposure using a photomask. After a post-exposure bake and a second flood exposure, the samples were developed in an organic solvent solution to reveal the pattern. An 80 nm gold layer was deposited via sputtering at a controlled rate of 1.05 nm s⁻¹. To complete the electrode, the unbound gold and photoresist were removed by lifting the membrane off in N-methylpyrrolidone. The membrane, now embedded with gold electrodes, was then released from the microscope slide by dissolving the PVA layer in water and dried at 60 °C. The microfluidic device was constructed from three polydimethylsiloxane (PDMS) layers. The apical and basolateral channels were created from 500 μm PDMS foils adhered to adhesives (ARcare® 90106NB) and precisely cut by xurography. A 3D-printed mold was used to cast the top layer, which served as a lid and medium reservoir. To ensure optical clarity for microscopy, an adhesive film (ARcare® 8259) was integrated into the mold as a window. PDMS prepolymer was mixed with a curing agent at a 10:1 ratio, degassed, poured into the mold, and cured at 60 °C for 6 hours. Following curing, the individual components were assembled. The apical PDMS layer and the top PDMS lid were plasma-bonded together, while the basolateral layer was bonded to a microscope slide. To ensure a permanent seal, these two assembled parts were incubated at 80 °C for at least 4 hours. To finalize the gut-on-a-chip system, the protective liners were removed from the adhesive layers, and the porous membrane containing the gold electrodes was carefully sandwiched and sealed between the apical and basolateral components.

2.2 HUMAN EPITHELIAL CELL LINES

Cell culture was conducted as previously described [2]. Briefly, to create an in vitro gut model that mimics certain aspects of the GIT, we used the colorectal adenocarcinoma cell lines Caco-2 (ATCC) and HT-29-MTX-E12 (ATCC). Standard cell culture reagents were acquired from Sigma-Aldrich. All cell culture experiments were carried out in a laminar flow hood at room temperature (RT) under sterile conditions. Media and other cell culture reagents were prewarmed at 37 °C or RT before usage. Caco-2 cells were maintained in minimum essential medium with Earl's salts (MEM; M0325) supplemented with 10% fetal bovine serum (FBS; F9665) and 1% antibiotics (AB; A5955) at 37 °C in a 5% CO₂ humidified atmosphere. The medium was changed every 2 or 3 days. To ensure biological repeatability, cells between passages 26-34 were split at 80-90% confluency, and experiments were conducted with cells with viability above 90%, as confirmed by Trypan Blue staining. HT-29-MTX-E12 cells were maintained in Dulbecco's modified Eagle's Medium (DMEM; D6429) supplemented with 10% fetal bovine serum (FBS; F9665) and 1% antibiotics (AB; A5955) at 37 °C in a 5% CO₂ humidified atmosphere. The medium was changed every 2 or 3 days. To ensure biological repeatability, cells with passage numbers 50-60 were split at 80-90% confluency, and experiments were conducted with cells with viability above 90%, as confirmed by Trypan Blue staining. THP-1 cells were maintained in Roswell Park Memorial Institute 1640 Medium (RPMI-1640; R8757) supplemented with 10% fetal bovine serum (FBS; F9665) and 1% antibiotics (AB; A5955) at 37 °C in a 5% CO₂ humidified atmosphere. The medium was changed every 2 or 3 days. To ensure biological repeatability, cells at passage numbers 40-50 were split to a concentration below 1×10^6 cells/mL, and experiments were conducted with cells with viability above 90%, as confirmed by Trypan Blue staining.

2.2.1 Cell Culture on and off-chip

Cell culture on and off-chip was performed as previously described [2]. The microfluidic devices were prepared for the on-chip cell culture experiment as follows: the channels and reservoirs were sterilised by wiping and priming with 70% ethanol, the platform was dried in a 60 °C oven, and it was subsequently exposed to UV for 30 min. To facilitate cellular adherence and differentiation, the chip membranes and TW systems with a 3 µm pore insert (662630, Greiner) were coated with 1% collagen type 1 (C3867) in a humidified incubator for 1 h, followed by flushing with complete media. Upon reaching 90% confluency, the cells were seeded onto the membranes at a density of 1.0×10^5 cells cm⁻² and grown for up to 14 days.

To demonstrate the system's versatility, we established both a direct co-culture of Caco-2 and HT29-MTX-E12 cells (7:3 ratio) and a tri-culture of Caco-2, HT-29-MTX-

E12, and THP-1 within TW systems and the microfluidic chip to improve the physiological relevance of the immune cells. Caco-2, HT29-MTX-E12 cells and THP-1 cells were cultured as previously described. Before the addition of the THP-1 cells to the intestinal co-culture, THP-1 cells were treated with 25nM PMA for 48 h to allow THP-1m differentiation. After 24h of recovery time and 6 days of intestinal co-culture, THP-1 cells were seeded at a density of 2.0×10^5 cells cm^{-2} into the basolateral compartment, and the tri-culture was maintained for an additional 4 days to allow equilibration.

2.3. Bacterial LPSs and membrane vesicles (BMVs)

We used one *E. coli* strain and one strain belonging to Bacteroidales as sources of pro-inflammatory and tolerogenic LPSs and BMVs, respectively. *E. coli* O26:B6 LPS was obtained from a commercial source (Sigma) and Bacteroidales LPS was extracted by using an in-house protocol and the numbering LPS and BMVs corresponds to the strain numbering defined in Deliverable 2.2. Briefly, the Bacteroidales strain was grown for 48h under anaerobic conditions and pelleted by centrifuging 4000rpm for 15min. The cell pellet was washed three times with a single-phase Bligh-Dyer with the LPS remaining in the insoluble fraction. The insoluble pellet was resuspended to endotoxin free water using 10-20ml volume depending on the size of the insoluble fraction. LPS concentration was measured with LAL assay (Pierce™ Chromogenic Endotoxin Quant Kit). BMVs, herein OMVs from gram-negative bacteria, were isolated as described previously [3]. The isolated BMVs were suspended in PBS and nanoparticle tracking analysis (NTA) was done in the EMV core facility of UH to quantify the BMVs. LPS and BMV isolations were performed by UH. Isolated BMVs were stored in -80°C until further usage for experimentation.

2.3 CHARACTERISATION OF THE INTESTINAL BARRIER INTEGRITY

OFF-CHIP

The following methods and materials for characterising barrier integrity on and off-chip were performed as previously described by Brandauer et al. [2] and briefly described in the following section.

2.3.1 Transepithelial Electrical Resistance Measurement within the TW system

The transepithelial electrical resistance (TEER) was measured using EVOM chopstick electrodes (STX-4 EVOM™, WPI). Cells were grown on 24-well Thincert membranes

coated with 1% collagen. TEER, which reflects the integrity of the Co-Culture monolayer, was measured during cultivation in the TW systems.

2.3.2 Impedance Measurement within the Microfluidic Platform

To monitor barrier formation by intestinal cells in the gut-on-a-chip platform, impedance was recorded daily. For measurements using the in-house-fabricated electrodes, the inlets and outlets of the microfluidic platforms were sealed with cell culture tape (236366PK, Thermo Fisher) and connected to a potentiostat (VMP3, Bio-Logic) via the contact pads of each electrode. Two-electrode electrochemical impedance-sensing measurements were performed with a sinusoidal amplitude of 10 mV, scanning from 1 MHz to 0.1 Hz. In order to analyse the barrier formation over time, the cell index (CI), introduced by *Pan et al.* [4] was calculated at approximately 20 kHz using the impedance signal of blanks without cells (Z_{blank}).

2.3.3 Diffusion Assay using FITC-Dextran

To assess cellular barrier permeability, a diffusion assay was performed using FITC-dextran (3–5 kDa, Sigma-Aldrich). This assay was conducted daily throughout the cultivation period on the microfluidic platform and the TW. Cell culture medium with 0.1 mg mL⁻¹ of fluorescence tracers was added to the apical channel and incubated for 60 minutes. Afterwards, the entire solution from the basolateral layer was sampled and measured using a plate reader (multimode plate reader, EnSpire 2300, PerkinElmer). Using a calibration curve, the FITC-dextran concentration in the basal channel was determined, enabling the calculation of the apparent permeability (Papp).

2.3.4 Aminopeptidase assay to evaluate enterocytic differentiation

To assess the functionality of differentiated Caco-2 intestinal cells, the specific activity of the brush border aminopeptidase enzyme was measured using an L-alanine-4-nitroanilide hydrochloride (A4N) assay on days 1, 3, and 7. This adapted assay from *Ferruzza et al.* [5] involves adding a reaction buffer containing 5 mM of the L-Ala-NA substrate to the apical channel of the microfluidic platform, while the basolateral channel is filled with PBS. The system was incubated for 20 minutes at 37 °C. Concurrently, a standard curve of the hydrolysis product, p-nitroanilide (p-NA), was prepared. After incubation, samples were collected from both channels and transferred to a 96-well plate. The absorbance of the produced p-NA was measured

at 405 nm using a plate reader. Blank values were subtracted, and the absorbance was converted to concentration using the standard curve. The final data, representing enzyme activity, were plotted as a function of time and cell culture area ($\text{nmol min}^{-1} \text{cm}^{-2}$).

2.3.5 Alcian blue staining to evaluate mucus production

To visualise acidic mucopolysaccharides (mucus), cells in both microfluidic and TW systems were fixed with 4% paraformaldehyde for 20 minutes at RT. The mucus was then acidified with 3% acetic acid for 3 minutes, rinsed with distilled water, and stained with alcian blue solution for 30 minutes. Finally, the cells were washed with PBS until the supernatant was cleared.

2.3.6 Immunocytochemistry of tight-junction marker ZO1

To evaluate tight junction formation in intestinal epithelial cells, zonula occludens-1 (ZO-1) immunostaining was performed during cultivation in the systems. Cells were first rinsed with PBS and then fixed with 4% paraformaldehyde (PFA) overnight at 4 °C. Following fixation, cells were permeabilised for 15 minutes using 0.2% Triton X-100 in PBS containing calcium and magnesium (PBS+). To prevent non-specific binding, samples were blocked for 2 hours with a solution of 1% BSA in PBS+. The cells were then incubated overnight at 4 °C with a rabbit polyclonal primary antibody against ZO1 (Proteintech®, 21773-1-AP) diluted at 1:200. After washing twice with PBS+, the cells were stained for 2 hours at RT with a goat anti-rabbit Alexa Fluor 555 secondary antibody (Invitrogen, A-32732) diluted at 1:1000. Nuclei were counterstained with DAPI (2 mg mL^{-1} , 1:1000 dilution) for 1 hour. Finally, the cells were washed once more with PBS+ before imaging. Fluorescence images were acquired with an Olympus IX83 microscope and subsequently processed in ImageJ.

2.4 PROINFLAMMATORY CAPACITY OF INFLAMMATORY CYTOKINE

14 days post-plating, the co-culture was switched to a starvation medium (without fetal bovine serum, FBS) for 24 h before inflammatory cytokine 1 (IC1) stimulation. The cells were then exposed to 50 ng/mL IC1 in the Basolateral side for 24 h to generate a chronic setting. Transepithelial electrical resistance (TEER) was measured before and 24 h after incubation of the barrier with IC1, using an EVOM2 TEER meter and an STX4 electrode (World Precision Instruments) to assess barrier integrity.

2.4.1 RNA isolation, cDNA synthesis and qPCR to analyse the TLR4 marker after Inflammatory cytokine treatment

Total RNA from both ICI-treated and untreated cells was extracted using an innuPREP RNA Mini Kit performed by UNICAM. RNA concentration was measured with a spectrophotometer and diluted to $44 \text{ ng } \mu\text{L}^{-1}$. Subsequently, $22 \text{ ng } \mu\text{L}^{-1}$ of RNA was reverse transcribed into cDNA using a high-capacity cDNA reverse transcription kit. For quantitative polymerase chain reaction (qPCR), $20 \text{ } \mu\text{L}$ reactions were prepared containing cDNA, specific primers, SYBR Green Master Mix, and nuclease-free water. The thermocycling protocol consisted of 40 cycles of $95 \text{ }^\circ\text{C}$ for 5 s and $60 \text{ }^\circ\text{C}$ for 30 s, following an initial 2-minute activation step. Amplification specificity was confirmed by melting curve analysis ($60\text{--}95 \text{ }^\circ\text{C}$). Relative gene expression was calculated using the $2^{(-\Delta\Delta\text{Ct})}$ method, with GAPDH serving as the housekeeping gene for normalisation.

2.5 PRO-INFLAMMATORY AND TOLEROGENIC CAPACITY OF LPS AND BMVs

Different concentrations of LPS and BMVs, consistent with those used by the Endotarget partner UH, were applied 10 days post-seeding of the tri-culture system (Caco-2, HT-29-MTX-E12, THP-1 cells) for durations ranging from three to 24 hours. Following incubation, the supernatants were collected. The levels of the proinflammatory cytokine IL-8 in these supernatants were measured using ELISA (BD Biosciences) and compared to medium controls. The experiments were conducted in two or three technical replicates.

2.6 LPS AND BMV COMPETITION ASSAY

2.6.1 Competition Assay with BMVs

Tolerogenic and inflammatory BMVs were incubated at a 1:10 ratio (10^8 BMVs in total) on the apical side of the tri-culture system for a period of 3–24 hours within an acute and chronic environment, the supernatants were collected and stored at $-20 \text{ }^\circ\text{C}$. ELISA was used to measure IL-8 levels. Controls included medium, from UH isolated inflammatory *E. coli* 2 BMVs (10^8 BMVs in total), and tolerogenic Bacteroidales 1 BMVs (10^8 BMVs in total).

2.6.2 Competition Assay with LPS

Tolerogenic and inflammatory LPS were incubated at a 1:10 ratio (100 ng/mL + 10 ng/mL) on the apical side of the tri-culture system for a period of 3-24 hours in an acute or chronic environment, as previously described. Supernatants were collected and stored at -20 °C, until IL-8 quantification by ELISA. Medium, from UH isolated inflammatory *E. coli* 2 LPS (10 ng/mL) and tolerogenic *Bacteroidales* 1 LPS (100 ng/mL) were used as controls.

3 RESULTS

3.1 ESTABLISHMENT OF THE EPITHELIAL BARRIER ON CHIP

3.1.1 Gut on a chip development with an integrated porous membrane-based impedance sensor

TUW developed a gut-on-a-chip system with integrated gold electrodes, comprising three PDMS layers – basal, apical and medium reservoir layer, as depicted in Figure 1A. The top view of the microfluidic system (Figure 1B) shows the three individual cultivation channels. The gold electrodes sputtered on PET membrane were sealed between the apical and basolateral PDMS foils using biocompatible adhesives. This platform has a cultivation area of 0.35 cm², making the results comparable to those of a 24-well ThinCerts® (0.34 cm²). To detect an average signal across the entire tissue, the electrodes cover 57% of the cultivation area. The sensor consists of two fingers with seven interdigitations each, which enables a two-electrode measurement configuration (Figure 1C). The final version of the chip was used as platform to test the proinflammatory effects of LPS or BMVs on the gut barrier in acute or chronic settings. This microfluidic chip provides a reliable electrical readout of barrier integrity that correlates with the gold-standard permeability assay.

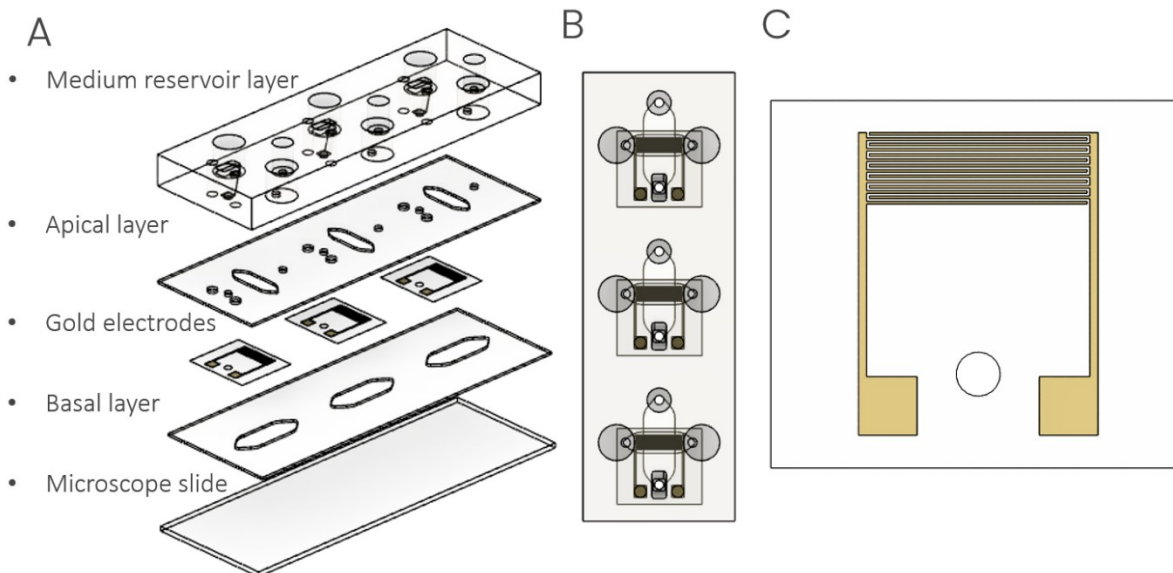


Figure 1: Schematics of the organ-on-a-chip model. (A) An exploded view and (B) a top view of the microfluidic system, showing the basolateral and the apical channels with three replicates, respectively. (C) Schematic illustration of the interdigitated gold electrode on a PET membrane.

3.1.2 Establishing the ratio of Caco-2 to HT-29-MTX-E12 for a co-culture model

Caco-2 human intestinal epithelial cells, which differentiate into polarised enterocytes are commonly used as an *in vitro* model of the intestinal lining, were combined with mucus-secreting HT-29-MTX-E12 cells to improve physiological relevance of the model. To identify the cell seeding ratio at which first, barrier permeability mainly coming from the Caco2 cells and second, mucus production mainly coming from the HT-29-MTX-E12 is not significantly compromised after 14 days, we evaluated barrier formation, permeability, mucus production, and ZO1 expression at three ratios (1:1, 7:3, and 9:1 Caco-2:HT29). The cells were seeded in commercial 24-Transwell systems and cultured for 14 days. TEER was measured with the EVOM STX-4.

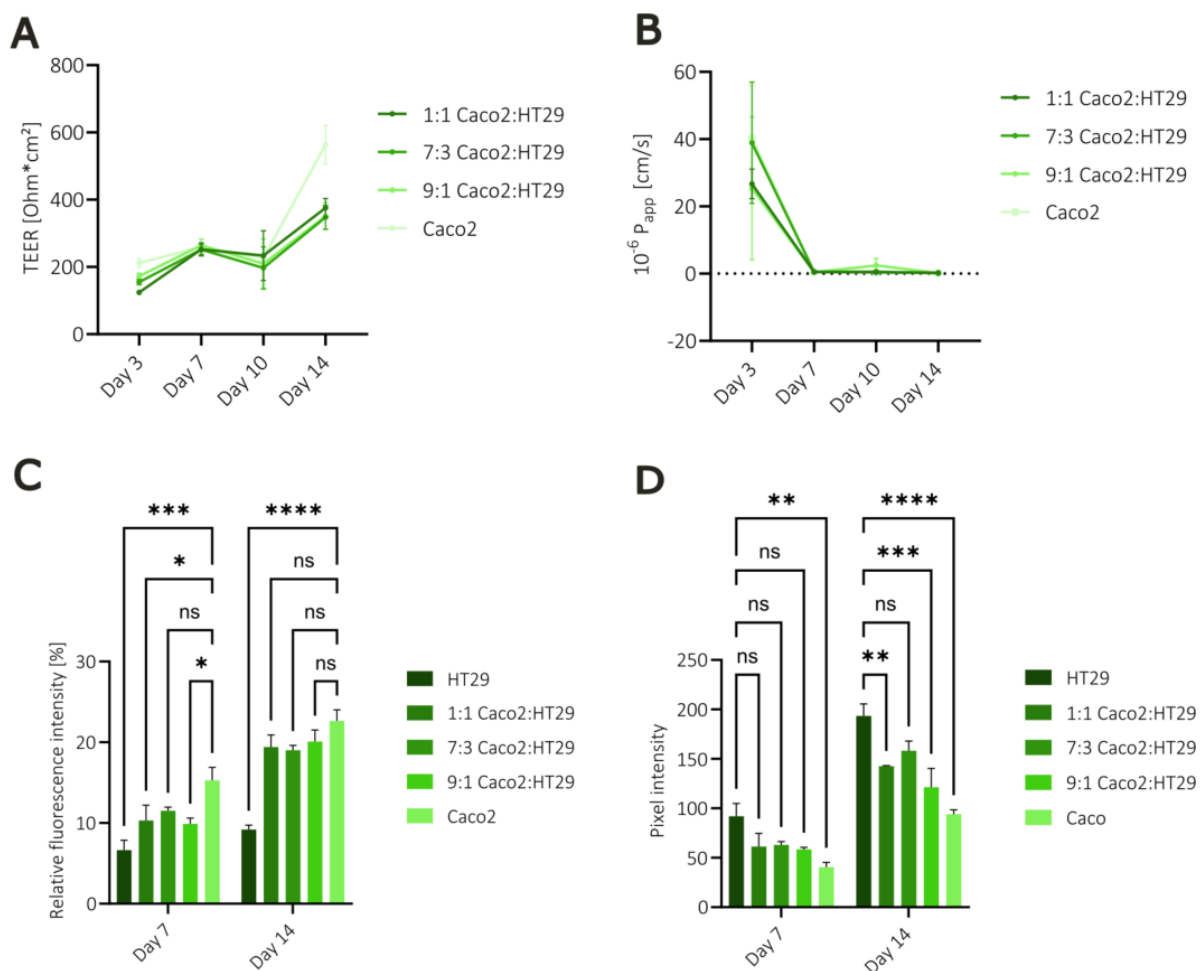


Figure 2: Establishing the epithelial co-culture ratio. (A) Transepithelial electrical resistance of the Caco-2 monoculture and the different cell seeding ratios of the co-culture with HT29 cells, revealing no difference between the ratios (N=3, mean with SD). (B) Apparent permeability of the mono and co-cultures over time (N=3, mean with SD). (C) Relative fluorescence intensity of ZO1 on day 7 and 14, normalised to the DAPI fluorescence intensity of the nuclei (N=3, mean with SD). (D) Pixel intensity of the mucus staining from the mono- and co-cultures after 7 and 14 days of cultivation (N=3, mean with SD).

All co-culture conditions formed an intermediate barrier with low permeability over 14 days, as indicated by TEER values ($300\text{--}400 \Omega \cdot \text{cm}^2$) and FITC-Dextran permeability (Papp of 10^{-6} cm/s). While the Caco-2 monoculture exhibited higher TEER, no significant differences were observed between the co-culture ratios for these metrics (Figures 2A & 2B). Immunocytochemistry stainings/assays confirmed that Caco-2 cells were the primary producers of the tight junction protein ZO-1, with HT29 cells expressing significantly less; co-cultures showed levels comparable to Caco-2 monocultures (Figure 2C). The primary differentiating factor was mucus production, which was highest in the HT29 monoculture and lowest in the Caco-2 monoculture. Critically, the 7:3 co-culture ratio produced significantly more mucus than the other ratios, reaching levels similar to the HT29 monoculture (Figure 3D).

In conclusion, the 7:3 Caco-2:HT29 ratio was selected for subsequent experiments. This condition generated a robust, low-permeability barrier, maintained high ZO-1 expression, and maximised mucus production, most closely replicating the key features of an *in vivo* intestinal epithelium.

3.1.3 Characterisation of the epithelial barrier on-chip

To demonstrate that the established TW *in vitro* cultivation protocol is applicable on-chip barrier formation, mucus staining and ZO-1 expression were monitored and compared to the TW conditions described in the previous chapter (3.1.2). To confirm barrier formation, impedance was measured daily, revealing an exponential increase in barrier integrity that plateaued by day 6, indicative of successful barrier formation (Figure 3A). This was further demonstrated by a FITC-dextran permeability assay, which showed an inverse correlation between apparent permeability (Papp). Furthermore, a Papp of $3.9 \pm 2.0 \times 10^{-6} \text{ cm/s}$ on day 7 indicated the formation of a tight barrier (Figure 3B). Immunofluorescence staining for ZO1 confirmed the presence of tight junctions and revealed a villi-like 3D architecture (Figure 3C). Figure 3D shows images of Alcian Blue-stained Caco-2 monoculture and Caco-2/HT29-MTX-E12 co-culture after 7 days on-chip, showing a dense mucus layer in both cultures. Pixel-intensity analysis of mucus staining revealed no significant differences between the two cultures, supporting robust mucus production in the co-culture and indicating/implying that the TW cultivation protocol is applicable in the on-chip scenario.

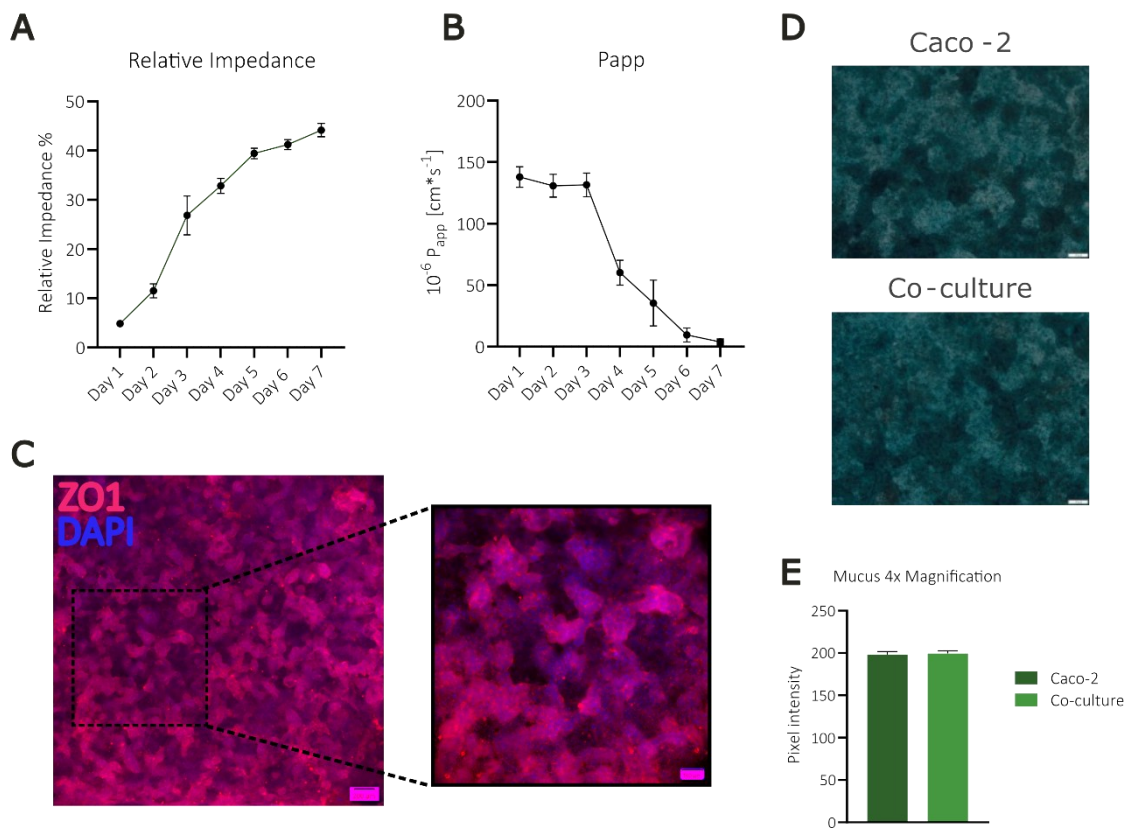


Figure 3: Evaluation of Caco2/Ht19-MTX on-chip co-culture. (A) Relative impedance values increase exponentially and plateau by day 6, indicating barrier formation (n=8). (B) Apparent permeability (Papp) decreases after day 3, reaching $3.9 \pm 2.0 \times 10^{-6} cm/s$ by day 7, consistent with enhanced barrier integrity (n=6). (C) Immunocytochemical staining for ZO-1 (red) and nuclei (blue, DAPI) shows uniform tight junction expression across the membrane (left, 4x) and 3D villi-like structures (right, 10x). Scale bars are 200 (left) and 100 μm (right). (D) Alcian blue staining of Caco-2 monoculture and Caco-2/HT29-MTX co-culture reveals a continuous mucus layer. Images were taken with a 4x magnification. Scale bars are 100 μm . (E) Quantification of mucus layer intensity

3.2 ESTABLISHING THE ACUTE AND CHRONIC INFLAMMATION SCENARIOS

After establishing the optimal ratio of Caco-2 and HT-29-MTX-E12 cells, we tested the pro-inflammatory effect of IC1 on the barrier function to mimic a chronic inflammation state. To assess the impact of inflammation on the co-culture barrier, we treated the barrier with IC1 for 24 hours, 15 days after plating and 24 hours after switching to starvation medium without FBS. The treatment caused a rapid and significant disruption of the epithelial barrier. As shown in Figure 4A, transepithelial electrical resistance (TEER), which measures barrier integrity, remained stable until Inflammatory cytokine exposure on day 15, after which it declined sharply and became statistically significant by day 16 (Figure 4B). The Co-cultured cells secreted the proinflammatory chemokine IL-8 in response to inflammatory cytokine stimulation, as shown in Figure 4C. A molecular response accompanied this functional

impairment; IC1 induced a time-dependent increase in TLR4 expression (Figure 4D). Notably, TLR4 gene expression of the coculture was significantly upregulated at 24 hours post-treatment compared to the untreated control. These findings demonstrate that IC1 effectively disrupts the physical barrier and concurrently primes epithelial cells for an enhanced response to bacterial components. Overall, these results illustrate the model's ability to replicate both the physical and molecular changes characteristic of intestinal inflammation.

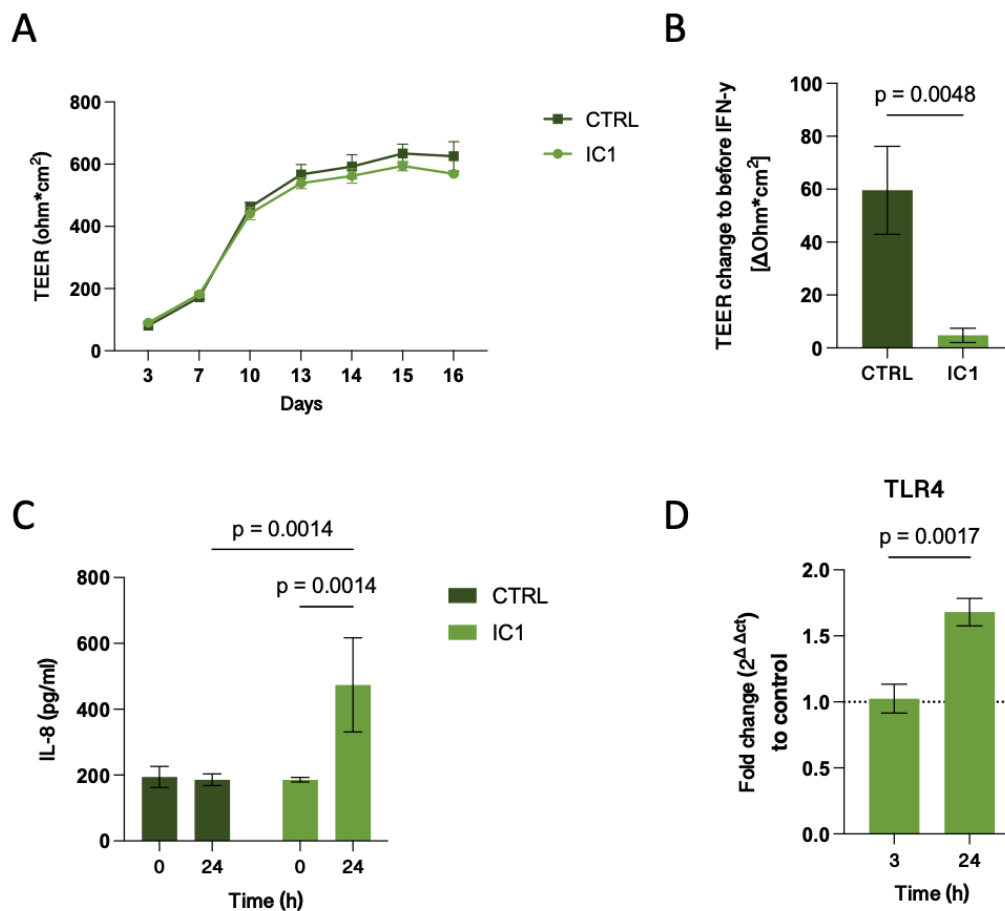


Figure 4: Establishing the acute and chronic scenario. (A) Transepithelial electrical resistance of the Co-Culture, revealing no difference between day 3 and day 15, and (B) a relative drop on day 16 after IC1 treatment. (N=3, mean with SD). (C) Induction of IL-8 release from the Co-culture after 24h stimulation with inflammatory cytokine, in comparison to without stimulation. (D) Gene expression of TLR4 of the Caco-2 and HT-29-MTX-E12 coculture, responsible for recognising bacterial LPS, 24h after Inflammatory cytokine treatment, visualised as fold change (n = 3, **P = 0.0031, ****P < 0.0001, ns are not shown). Statistical analyses were conducted using a two-way ANOVA and a Sidak's multiple comparison test.

3.3 EFFECT OF LPS AND BMVs ON THE BARRIER INTEGRITY ON AND OFF-CHIP

To establish the final tri-culture setup for the competition assays, we initially planned to add endothelial cells, however, in order to improve the immunological response we decided to create a tri-culture protocol in which we added macrophages differentiated from THP-1 cells (THP-1m).

3.3.1 Effect of BMVs on Barrier Integrity with THP-1m off-chip

After establishing the tri-culture off-chip, we tested the effect of proinflammatory and tolerogenic BMVs on the tri-culture. We tested the simultaneous impact of both proinflammatory and tolerogenic BMVs on the tri-culture. THP-1-derived macrophages (THP-1m) were introduced into the basolateral compartment of the TW system after 6 days of intestinal co-culture. Cells were maintained for additional 4 days to allow equilibration. Before the addition of BMVs, the tri-culture was primed with inflammatory cytokines to simulate a chronic environment. BMVs from the proinflammatory *E. coli* 2 and the tolerogenic Bacteroidales 1 provided by UH were applied in a 1:10 ratio to the apical compartments to repeat and extend the competition assay described by UH (D2.2 and D2.3), focusing on the impact of a single potent strain. *E. coli* 2 alone was applied as a control.

TEER was measured 24 hours post-BMV treatment. A drop in TEER was observed between the two groups, indicating an effect of the inflammatory cytokine on barrier integrity. However, the impact of BMVs within the groups were similar, resulting in no visible effect of the BMVs on the barrier integrity (Figure 5A). FITC-dextran permeability was assessed after 24 hours of BMV treatment. Unexpectedly, permeability was similar within the groups and across the acute and chronic settings (Figure 5B).

The BMVs, both inflammatory and tolerogenic, were further tested in an in vitro cell culture model for IL-8 release (Figure 5C). In both acute and chronic settings, there was no difference after BMV treatment. However, across the acute and chronic settings, IL-8 was increased within the chronic setting, indicating an effect of the proinflammatory cytokine. The results suggest that the effect of inflammatory cytokine mirroring the chronic exposure has a strong effect on barrier function and inflammatory response but the stimulation with BMVs had no significant effect on the measured parameters at the chosen timepoint neither in acute nor chronic condition on off-chip assay.

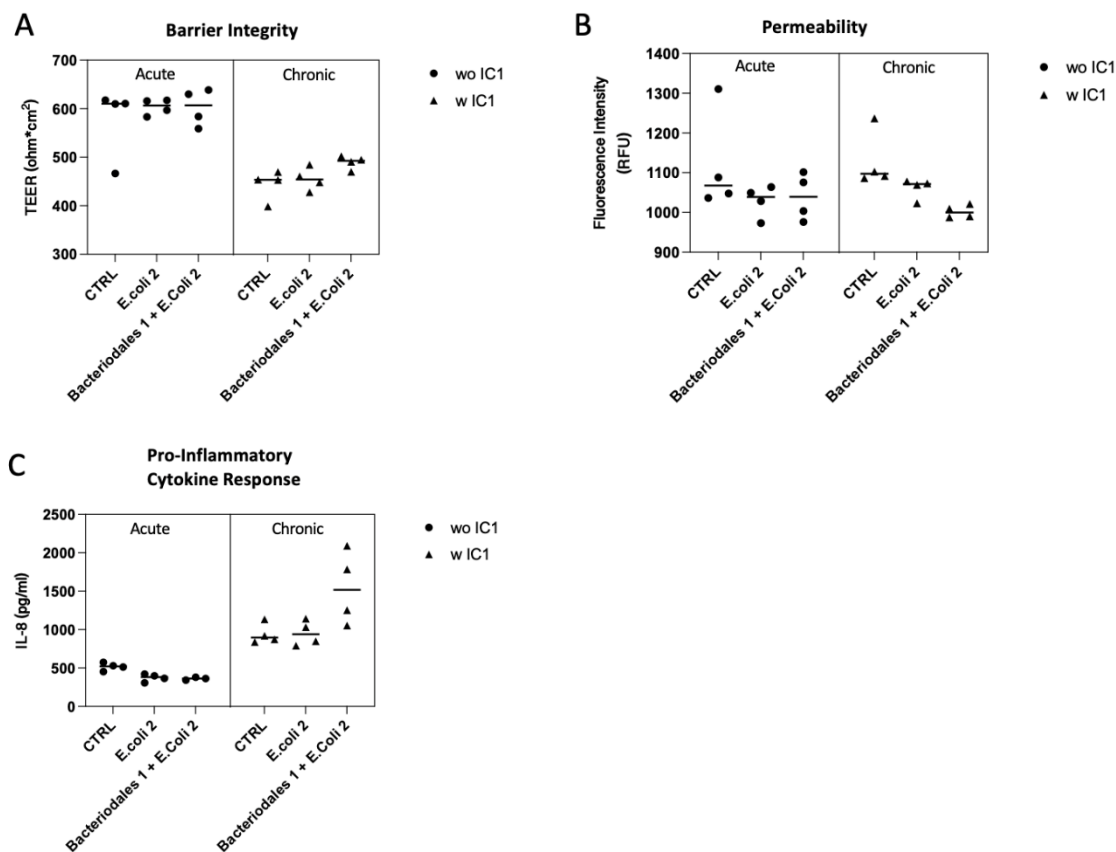


Figure 5: Effect of RD-associated and tolerogenic BMVs in an acute and chronic off-chip setup. (A) Barrier integrity was assessed by measuring transepithelial electrical resistance (TEER) in epithelial monolayers under acute and chronic conditions. Treatments included control (CTRL), E. coli 2, Bacteroidales 1 + E. coli 2*, with or without IC1. (B) Permeability was evaluated by the fluorescence intensity (RFU) of a tracer molecule (FITC Dextran 3-5kDa) passing through the epithelial barrier. (C) The pro-inflammatory cytokine response was measured as IL-8 secretion (pg/mL) in cell culture supernatants.

3.3.2 Effect of BMVs on Barrier Integrity with THP-1m on-chip

After establishing the tri-culture system off-chip, we investigated the effects of pro-inflammatory and tolerogenic BMVs on the intestinal epithelial barrier using a microfluidic chip model. We examined the impact of BMVs from pro-inflammatory E. coli 2 and tolerogenic Bacteroidales 1 (isolated by UH) on the system. THP-1-derived macrophages (THP-1m) were added to the basolateral compartment after 6 days of co-culture and kept for 4 days for equilibration. BMVs were then applied at 1:10 ratio to the apical compartments, mimicking a previous competition assay and assessing a single strain (E. coli 2). FITC-dextran permeability was measured after 24 hours; permeability was similar across groups, regardless of BMV type (Figure 6A). IL-8 secretion, a marker of inflammation, was also evaluated. IL-8 levels were significantly higher with the BMV mixture than with pro-inflammatory BMV alone, indicating no tolerogenic effect for Bacteroidales 2 (Figure 6B).

These findings suggest that BMVs do not weaken barrier integrity but rather increase pro-inflammatory signaling, indicating that they affect gut epithelial cells.

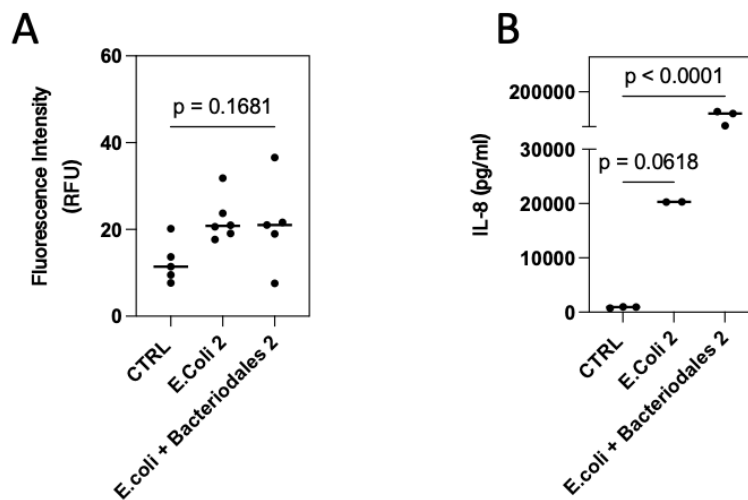


Figure 6: Effect of RD-associated and tolerogenic BMVs in an acute on-chip setup. (A) Permeability was evaluated by the fluorescence intensity (RFU) of a tracer molecule (FITC Dextran 3-5kDa) passing through the epithelial barrier. (B) The pro-inflammatory cytokine response was measured as IL-8 secretion (pg/mL) in cell culture supernatants.

3.3.3 Effect of LPS on Barrier Integrity with THP-1m off-chip

After establishing the tri-culture off-chip, we tested the effect of proinflammatory and tolerogenic LPS on the tri-culture. We tested the simultaneous impact of both proinflammatory and tolerogenic LPS on the tri-culture. THP-1m were introduced into the basolateral compartment of the TW system after 6 days of intestinal co-culture. Cells were maintained for an additional 4 days to allow equilibration. Before the addition of LPS, the triculture was primed with inflammatory cytokines to simulate a chronic inflammatory environment. LPS from the pro-inflammatory E. coli 2 and the tolerogenic Bacteroidales 1 provided by UH were applied in a 1:10 ratio to the apical compartments to repeat and extend the competition assay described by UH focusing on the impact of a single potent strain. E. coli 2 alone was applied as a control.

TEER was measured 24 hours post-LPS treatment. The observed TEER values of the chronic inflammation condition were lower compared to the acute inflammation condition indicating an effect of the inflammatory cytokine on barrier integrity. However, the impact of LPS within the groups were similar, resulting in no visible differences between pro-inflammatory, tolerogenic LPS's and the competitive stimulations on the barrier integrity (Figure 7A). FITC-dextran permeability was assessed after 24 hours of LPS treatment. Unexpectedly, permeability was similar within the groups and across the acute and chronic settings (Figure 7B).

The LPS, both inflammatory and tolerogenic, were further tested in an in vitro cell culture model for IL-8 release (Figure 7C). In both acute and chronic settings, LPS treatments did

not differ from mock treatment. However, across the acute and chronic settings, IL-8 secretion was increased in the chronic setting, indicating an additive effect on the proinflammatory cytokine. The results suggest that exposure to LPS has differential effects on barrier function and inflammation under acute and chronic exposure conditions.

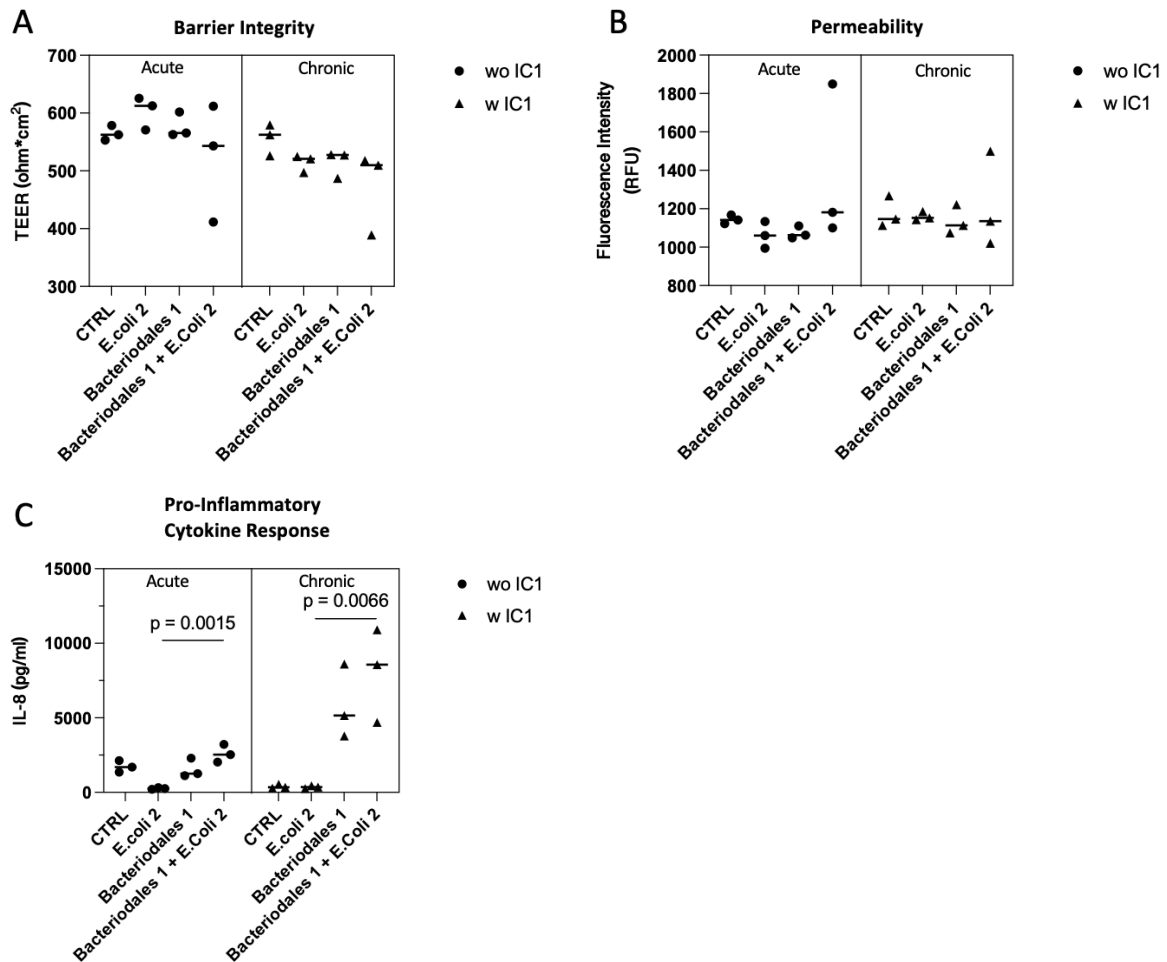


Figure 7: Effect of RD-associated and tolerogenic LPS in an acute and chronic off-chip setup. (A) Barrier integrity was assessed by measuring transepithelial electrical resistance (TEER) in epithelial monolayers under acute and chronic conditions. Treatments included control (CTRL), E. coli 2, Bacteroidales 1 + E. coli 2*, and Bacteroidales 1 + E. coli 2* with or without IC1. (B) Permeability was evaluated by the fluorescence intensity (RFU) of a tracer molecule (FITC Dextran 3-5kDa) passing through the epithelial barrier. (C) The pro-inflammatory cytokine response was measured as IL-8 secretion (pg/mL) in cell culture supernatants.

3.3.4 Effect of LPS on Barrier Integrity with THP-1m on-chip

After establishing the tri-culture system off-chip, we investigated the effects of pro-inflammatory and tolerogenic LPS on the intestinal epithelial barrier in a microfluidic chip model. We examined the impact of LPS from pro-inflammatory E. coli 2 and tolerogenic Bacteroidales 1 (UH) on the system. THP-1-derived macrophages (THP-1m) were added to the basolateral compartment after 6 days of co-culture and kept for 4 days for equilibration. In the chronic setup, a pro-inflammatory cytokine was added 24 h

pre-LPS, which was then applied at a 1:10 ratio to the apical compartments, mimicking a previous competition assay described by UH (D2.2). Two single strains (*E. coli* 2 and Bacteroidales 1) were assessed. FITC-dextran permeability was measured after 24 hours; permeability was similar across groups, regardless of LPS type (Figure 8A). IL-8 secretion, a marker of inflammation, was also evaluated as shown in Figure 8B. The IL-8 levels were significantly higher with the LPS single strain Bacteroidales 1 and the mixture of both the pro-inflammatory and tolerogenic strains, indicating no tolerogenic effect for Bacteroidales 2 (Figure 8B).

These findings suggest that LPS do not compromise barrier integrity but rather enhance pro-inflammatory signalling, indicating they affect gut epithelial cells. The difference between the acute and chronic states is minimal, suggesting no increase in the pro-inflammatory effect of the LPS on the barrier.

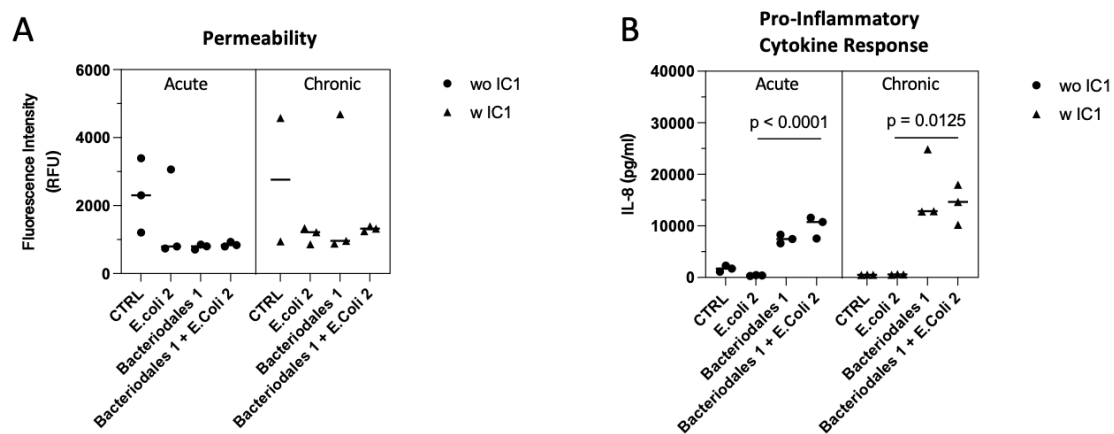


Figure 8: Effect of RD-associated and tolerogenic LPS in both acute and chronic on-chip setup. (A) Permeability was evaluated by the fluorescence intensity (RFU) of a tracer molecule (FITC Dextran 3-5kDa) passing through the epithelial barrier. (B) The pro-inflammatory cytokine response was measured as IL-8 secretion (pg/mL) in cell culture supernatants.

3.3.5 Longitudinal study on-chip of LPS exposure on intestinal tri-culture barrier integrity and immune response

To elucidate if the on-chip platform is capable to investigate longitudinal changes upon addition of RD-associated LPS on the Tri-culture system, the endpoint methods such as permeability, IL-8 concentrations were compared to the changes in impedance over time. There the THP-1 cells were introduced into the basolateral compartment to assess the immune response and barrier integrity of the intestinal co-culture following exposure to 100 ng/mL LPS *E.coli* 2. Impedance was measured every 3 hours over 5 days, revealing no substantial effect of LPS on barrier integrity (Figure 9A). A transient increase in impedance was observed after medium exchange, which might be attributed to temperature fluctuations affecting the measurement. To validate the barrier function, a FITC-dextran permeability assay was conducted at the end of the experiment, revealing no significant difference

between the untreated and LPS-treated tri-culture (Figure 9B). Additionally, supernatants from the apical and basolateral compartments were collected on days 2 and 5 for IL-8 quantification (Figure 9C). The untreated tri-culture exhibited low IL-8 levels that slightly increased over time, probably due to extended serum-free cultivation. Within the LPS-treated intestinal cell compartment, IL-8 levels on days 3 and 5 were significantly lower than in the underlying THP-1m cell compartment, with immune responses intensifying over time in both compartments. Although immune cells responded to LPS by elevating IL-8 secretion, no impact on barrier integrity was observed even after 5 days of exposure. The permeability and IL-8 concentrations in longitudinal study on-chip study describe a difference that was not monitored in the previous on-chip study presented in figure 8, which could be attributed to the presence of the electrodes on the PET membrane and an associated change in cellular expression.

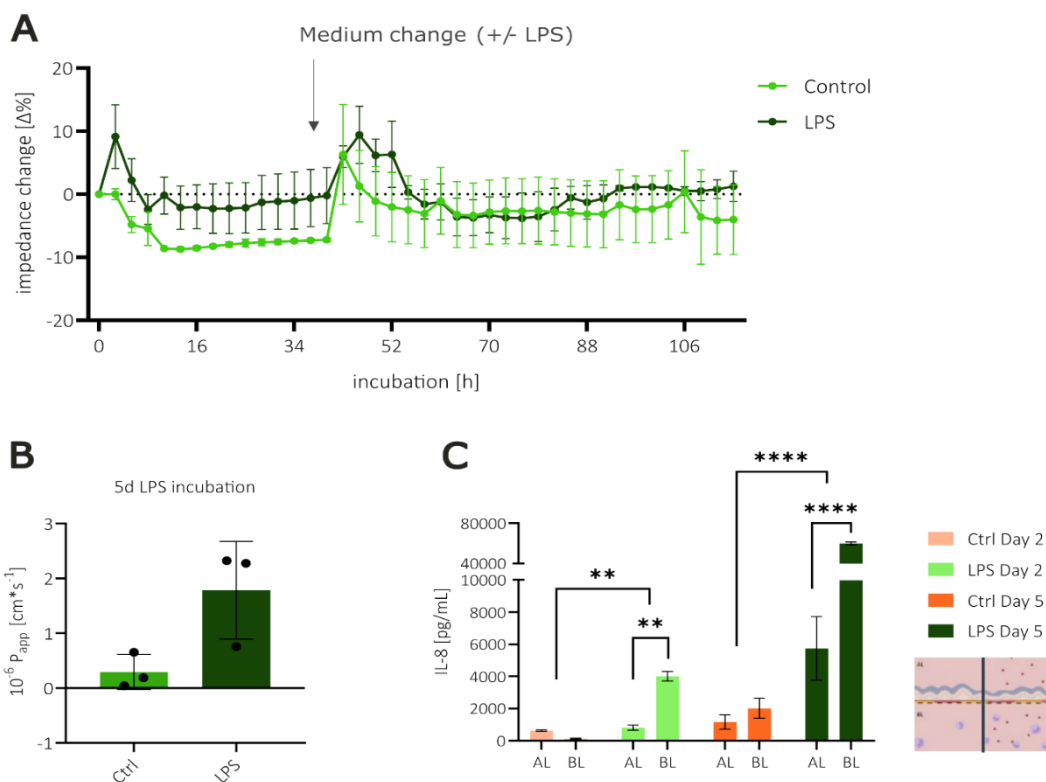


Figure 9: Impact of LPS exposure on intestinal tri-culture barrier integrity and immune response. (A) Impedance measurements over 5 days of LPS exposure (100 ng/mL) show no significant disruption of barrier integrity compared to control (n=4), with a transient increase observed after medium change due to temperature effects. (B) The FITC-dextran permeability assay performed after 5 days confirms no significant differences in P_{app} between control and LPS-treated tri-cultures (n=3). (C) IL-8 concentrations in apical (AL) and basolateral (BL) supernatants sampled on day 2 and day 5. LPS-treated cultures exhibit significantly higher IL-8 secretion than controls, especially on day 5, indicating a time-dependent immune response (n=3). The schematic illustration shows the compartmental setup for cytokine sampling.

4 CONCLUSIONS

Here we demonstrated the development of the microfluidic gut-on-a-chip platform with integrated impedance sensing to study the effects of bacterial-derived compounds on intestinal barrier integrity in acute and chronic inflammation settings. The triple-coculture model, comprising Caco-2, HT-29-MTX-E12, and THP-1-derived macrophages, successfully recapitulates key features of the intestinal environment, including mucus production, tight junction formation, and immune interactions. While permeability testing, TEER and impedance-based measurements provided valuable insights into the barrier formation process, their inconclusive nature to differentiate between acute and chronic state underscored the critical role of complementary cytokine quantification as performed using an IL-8 ELISA. Our findings demonstrate that the inflammatory cytokine 1 disrupts barrier function and elevates inflammatory cytokine expression, allowing its use as model to differentiate between acute and chronic inflammation settings.

In the off-chip competition assay between tolerogenic Bacteroidales and pro-inflammatory E. coli, neither their LPS nor bacterial membrane vesicles (BMVs) show a conclusive trend in compromising barrier integrity under the tested conditions. However, both LPS and BMVs induced significant pro-inflammatory responses, evidenced by increased IL-8 secretion, highlighting their role in immune activation. It became evident that competition assays using bacterial membrane vesicles (BMVs) exhibited minimal impact on IL-8 secretion differences, prompting a focused evaluation of lipopolysaccharides (LPS) as key drivers of inflammatory pathways.

The on-chip competition assays confirmed the trends observed in the off-chip setups. In the final experiments, it was demonstrated that the organ-on-chip system is a platform that allows for longitudinal assessments of barrier function, permeability testing and metabolite profiling.

These results underscore the key role of immune-epithelial crosstalk in endotoxemia and provide a foundation for therapeutic strategies targeting microbial-host interactions in rheumatic diseases. Future work should explore combinatorial effects of microbial metabolites, dietary interventions, and pharmacological agents to mitigate inflammation and restore barrier homeostasis.

5 REFERENCES

- [1] P. Schuller *et al.*, "A lab-on-a-chip system with an embedded porous membrane-based impedance biosensor array for nanoparticle risk assessment on placental Bewo trophoblast cells," *Sensors and Actuators B: Chemical*, vol. 312, p. 127946, June 2020, doi: 10.1016/j.snb.2020.127946.
- [2] K. Brandauer *et al.*, "Sensor-integrated gut-on-a-chip for monitoring senescence-mediated changes in the intestinal barrier," *Lab Chip*, vol. 25, no. 7, pp. 1694–1706, Mar. 2025, doi: 10.1039/D4LC00896K.
- [3] K. Hiippala *et al.*, "Novel *Odoribacter splanchnicus* Strain and Its Outer Membrane Vesicles Exert Immunoregulatory Effects *in vitro*," *Front. Microbiol.*, vol. 11, Nov. 2020, doi: 10.3389/fmicb.2020.575455.
- [4] Y. Pan *et al.*, "3D cell-based biosensor for cell viability and drug assessment by 3D electric cell/matrigel-substrate impedance sensing," *Biosensors and Bioelectronics*, vol. 130, pp. 344–351, Apr. 2019, doi: 10.1016/j.bios.2018.09.046.
- [5] S. Ferruzza, C. Rossi, M. L. Scarino, and Y. Sambuy, "A protocol for *in situ* enzyme assays to assess the differentiation of human intestinal Caco-2 cells," *Toxicology in Vitro*, vol. 26, no. 8, pp. 1247–1251, Dec. 2012, doi: 10.1016/j.tiv.2011.11.007.